JOURNAL OF AGRICULTURAL AND FOOD CHEMISTRY

Biodegradation of Oak (*Quercus alba*) Wood during Growth of the Shiitake Mushroom (*Lentinula edodes*): A Molecular Approach

CHRISTOPHER H. VANE,*,† TREVOR C. DRAGE,‡ AND COLIN E. SNAPE‡

British Geological Survey, Kingsley Dunham Centre, Keyworth, Nottingham NG12 5GG, United Kingdom, and School of Chemical, Environmental and Mining Engineering, University of Nottingham, NG7 2RD, United Kingdom

The chemical transformations that occur during growth of the shiitake mushroom (*Lentinula edodes*) on oak (*Quercus alba*) were investigated to improve mushroom cultivation and utilization of the spent substrate. Oak logs were decayed by *L. edodes* over 8 years, during which time they were sampled at six intervals (30, 40, 66, 76, 77, and 101 months). Fresh and decayed oak samples were analyzed using solid-state ^{13}C NMR and pyrolysis−gas chromatography−mass spectrometry as well as off-line thermochemolysis with tetramethylammonium hydroxide. Degraded oak exhibited lower carbon contents and increased oxygen content compared to the control. Solid-state ^{13}C NMR analysis revealed that polysaccharides were the major component of both fresh and decayed oak but that *L. edodes* mediated the preferential loss of cellulose and xylans as compared to lignin, which remained in an altered form. Several trends point toward the degradation of lignin, including a decrease in the proportion of syringyl units as compared to guaiacyl units and a reduction in side-chain length. An increase in guaiacyl and syringyl acid-to-aldehyde ratios occurred with growth, which suggested that the fungus had caused oxidation of Cα−Cβ bonds. The overall effect of *L. edodes* on oak is similar to that of many white-rot fungi, which simultaneously degrade all cell wall components.

KEYWORDS: Lignin; polysaccharide; degradation; shiitake mushroom; *Lentinula edodes*; thermochemolysis, pyrolysis; solid-state ^{13}C NMR; *Quercus alba*; oak

INTRODUCTION

The shiitake mushroom, *Lentinula edodes*, is widely cultivated on oak logs under natural environmental conditions. White-rot, basidomycete fungi degrade lignin, the mainly ether-linked phenylpropanoid biopolymer found in wood cells, either selectively or in parallel with polysaccharides (*1*). Multiple enzymes are involved in wood decay; these attack wood constituents either directly or indirectly by low-molecular-weight mediators (*1*). The detection of the enzyme manganese peroxidase, which catalyzes lignin degradation and the protein laccase, which directly oxidizes lignin, confirmed that *L. edodes* had appreciable lignin-degrading potential (*2, 3*). The mechanism of lignin decay induced by *L. edodes* has been investigated using model compounds. Manganese peroxidase, extracted from extracellular fluid of shiitake mycelium, degraded the model compounds vanillyl and veratryl alcohols via side-chain oxidation, aromatic ring cleavage, and methoxyl demethylation (*4*, *5*). It was reported in an additional study that 2,4-dihydroxy-3,3-dimethoxy-5-methyldiphenylmethane was decayed via oxidative cleavage of the side chain. In contrast, non-phenolic 5,5′-biphenyl and 5,5′-diphenylmethane were found to be unreactive to manganese peroxidase extracted from *L. edodes*, as demonstrated by gas chromatography−mass spectrometry (GC-MS) (*6*).

Lignin decomposition during solid-state fermentation with *L. edodes* has been investigated by phosphylitization of fresh and decayed wheat lignin using ^{31}P NMR spectroscopy (*7*). The biologically altered lignin was decomposed via stereoselective side-chain oxidation, as suggested by a decrease in the erythro/threo ratio. The NMR spectra also revealed a greater increase in carboxylic acid groups as compared to aliphatic hydroxyl groups and a decrease in phenolic moieties, which suggested that aromatic ring-cleavage reactions had also occurred during fungal attack. It was also suggested, on the basis of an increase in ^{1}H NMR resonances at ∼0.8 and 1.3 ppm, which can be assigned to aliphatic protons, that reductive reactions had occurred upon fungal biodegradation (*7*). Comparison of the chemical structure of acetylated lignin from *Triticum aestivum* (wheat) and oak (*Quercus robur*) using ^{13}C NMR spectroscopy has revealed that the interunit linkages in wheat lignin are significantly different from those in oak (*8*). Therefore, analysis of hardwood logs is required to elucidate the changes that occur during growth of shiitake mushrooms. We have carried out the

* Corresponding author (telephone +44-0115 936 3017; fax +44-0115 936 3460; E-mail chv@bgs.ac.uk).
† British Geological Survey.
‡ Univeristy of Nottingham.

10.1021/jf020932h CCC: $25.00
Published on Web 01/14/2003

compositional characterization of white oak (*Quercus alba*) logs which are used widely in the United States for shiitake cultivation.

Past evaluation of wood decay during growth of *L. edodes* has been limited; one study investigated the effect of decomposition using infrared spectroscopy and pyrolysis−gas chromatography−mass spectrometry (Py-GC-MS). Both analytical methods revealed a slight preferential removal of lignin as compared to polysaccharides after 98 days of biodegradation. However, no mushrooms were grown in the laboratory-based study (*9*). Monitoring the chemical composition of oak could aid in the optimization of shiitake production and commercial exploitation of the degraded logs as compost. This investigation used solid-state ^{13}C NMR, analytical pyrolysis, and thermochemolysis in the presence of tetramethylammonium hydroxide to characterize the molecular changes that occur in white oak as a function of cultivation time during commercial production of *L. edodes*.

MATERIALS AND METHODS

Cultivation of *L. edodes*. Healthy white oak trees (*Quercus alba*) grown within a 5-mile radius of Shirley, Arkansas, were cut into logs approximately 90 cm long and 10−15 cm in diameter. The moisture content of each log was maintained at ∼35% (w/w) by the addition of water. Inoculation was achieved by drilling 30 holes of depth ∼2.5 cm in a diamond pattern and packing with fresh spawn of *L. edodes*. After completion of the spawn run (6 months), the colonized logs were placed outside (natural fruiting 2−3 times per year); the temperature range was 7.2−21.1 °C. Samples of oak sapwood (∼5 g dry weight) were removed at 0, 30, 40, 66, 76, 77, and 101 months. Each sample was washed with sterile distilled water to remove surface mycelium and freeze-dried to remove water.

General. The authentic standards 4-methoxyacetophenone, 3,4-dimethoxybenzaldehyde, 3,4-dimethoxyacetophenone, 1,2,3-trimethoxyphenol, 3,4,5-trimethoxybenzaldehyde, and 3,4,5-trimethoxyacetophenone and the internal standard *n*-eicosane were reagent grade (Sigma-Aldrich Chemical Co., Gillingham, Dorset, U.K). Fresh and fungally decayed oak woods were powdered to pass through a 63-μm sieve, extracted in a Soxhlet apparatus with CH_2Cl_2 for 24 h, and dried under vacuum with P_2O_5.

Elemental Analysis. The organic carbon, hydrogen, and nitrogen content of oak samples was determined in quadruplicate using a Carlo Erba 1106 elemental analyzer. Ash content was determined gravimetrically following combustion of the dry powdered oak at 650 °C for 18 h (*10*). Blanks and samples were interchanged in order to account for possible instrumental drift.

Bulk Carbon Isotope Analysis. Stable carbon isotopic compositions for dried and powdered oak woods were determined using a Carlo Erba NA1500 elemental analyzer for on-line combustion (oxidation furnace setting 1020 °C; reduction furnace setting 650 °C). CO_2 and N_2 were separated by gas chromatography prior to analysis using a Micromass Optima gas source isotope ratio mass spectrometer. The $^{13}C/^{12}C$ ratio of the organic carbon in each wood sample is reported relative to PDB carbonate standard using the δ ^{13}C (‰) notation; a second internal cellulose standard (sigmacell, Sigma Chemical Co.) was used to account for instrumental drift. Based upon replicate analyses, the analytical error for the oak woods was ±0.2‰, and that for the authentic cellulose standard was <±0.1‰.

Pyrolysis−Gas Chromatography−Mass Spectrometry. Fresh and fungally decayed oak wood samples (0.5−0.7 mg) were placed in borosilicate glass tubes (Clark Electro Chemicals), and both ends of the tubes plugged with pre-extracted silica wool. Pyrolysis−gas chromatography−mass spectrometry (Py-GC-MS) was performed in a flow of helium using a Girdel 75-PY-1 pyrolyzer unit, fitted with a platinum coil connected to a Fisons 8000 series gas chromatograph (GC). The platinum coil was heated for 20 s at 600 °C, as measured by a thermocouple in the sample holder. Volatile products were separated using a 30-m × 0.25-mm-i.d. Chrompack CP-Sil 8 fused silica column (film thickness 0.25 μm). The GC oven was operated using the following program: isothermal for 5 min at 40 °C, then raised from 40 to 300 °C at 4 °C/min and held isothermally at 300 °C for 10 min with helium as the carrier gas. The GC was directly coupled to a Fisons MD800 mass spectrometer operated at 70 eV with a mass range of *m*/*z* 30−550, trap current 140 μA, and source temperature 270 °C. Data acquisition and analysis were performed using a Mass Lab data system. Products were tentatively identified by comparison of their mass spectra and relative retention times with those of compounds reported in the literature (*11*) and the National Institute of Standards library (NIST).

Pyrolysis Parameters. The syringyl/guaiacyl ratio (S/G) was calculated by dividing the sum of the peak areas of syringyl units by the sum of the peak areas of guaiacyl units. The guaiacyl phenylpropane/guaiacyl parameters (G:3/G) were measured using peak areas of the cis and trans isomers of 2-methoxy-4-(prop-2-enyl)phenol and 2-methoxy-4-(propan-2-one)phenol as well as 2-methoxy-4-(prop-2-enal)-phenol to the sum of guaiacyl units. The syringyl phenylpropane/syringyl ratio (S:3/S) was calculated by dividing the sum of 2,6-dimethoxy-4-(prop-1-enyl)phenol, the two isomers of 2,6-dimethoxy-4-(prop-2-enyl)phenol, 2,6-dimethoxy-4-(propan-2-one)phenol, 2,6-dimethoxyphenol-4-(propan-3-one), 2,6-dimethoxy-4-(prop-1-en-3-one), and 2,6-dimethoxy-4-(prop-2-enal)phenol by the sum of syringyl pyrolysis products.

Off-Line Thermochemolysis. For each experiment, borosilicate glass tubing (o.d. 5 mm, i.d. 4 mm), was sealed at one end with a natural gas/oxygen flame to give a vessel of length 13 cm. Each vessel was rinsed with methylene chloride and oven-dried for 12 h at approximately 75 °C. Fresh and fungally decayed spruce wood samples (0.5−1 mg) were placed in individual reaction vessels with 100 μL of tetramethylammonium hydroxide (TMAH) solution (25% w/w in methanol). The TMAH preparations were left overnight in a vacuum desiccator in the presence of P_2O_5 in order to facilitate thorough mixing prior to the removal of methanol under vacuum. The dried mixtures were sealed under vacuum and heated in an oven at 250 °C for 30 min. After cooling, the reaction vessels were opened, and the inner surfaces of the tubes were washed five times with 1 mL of dichloromethane. The combined extracts were dried under a stream of N_2 and dissolved in 100 μL of dichloromethane.

Gas Chromatography−Mass Spectrometry. GC-MS was performed using a Fisons MD-800 operated at 70 eV with a mass range of *m*/*z* 30−600 with helium carrier gas. The GC was fitted with a 30-m × 0.2-mm-i.d. HP-5 fused silica column coated with a 5% phenylmethylsilicone-bonded stationary phase (film thickness 0.25 μm). The oven temperature was programmed from 30 to 300 °C at 4 °C/min and held isothermally at 300 °C for 5 min.

Thermochemolysis Parameters. The compound labels (G and S) denote structures shown in **Figure 1**. Acid/aldehyde $(Ad/Al)_G$ parameters were measured using peak areas of G6 and G4 [$(Ad/Al)_G$ = G6/G4] as well as methyl 3,4,5-trimethoxybenzoate (S6) and 3,4,5-trimethoxybenzaldehyde (S4) [$(Ad/Al)_S$ = S6/S4]. The syringyl/guaiacyl ratio $(S/G)_{TMAH}$ was calculated by dividing the sum of the peak areas from syringyl derivatives (S4−S16) by the sum of the peak areas from their guaiacyl counterparts (G4-G16). The Γ parameter was determined from the ratio of G6 to the sum of the peak areas of *threo*-/*erythro*-1-(3,4-dimethoxyphenyl)-1,2,3-trimethoxypropane (G14 and G15).

Solid-State ^{13}C Nuclear Magnetic Resonance. Solid-state ^{13}C NMR spectra were obtained for fresh and degraded oak samples using a Bruker DSX200 instrument equipped with double-bearing probes for cross polarization (CP) and magic angle spinning (MAS). The resonance frequency for ^{13}C was 50 MHz, and the sample was spun at the magic angle with a speed of 6.0 kHz. Typically 10 000 scans were accumulated with high-power ^1H decoupling for the CP experiments. For CP, the contact time was 3.0 ms, and the relaxation delay was 1.5 s. Dipolar dephasing experiments were carried out using a dephasing period of 50 μs. All spectra were obtained at ambient temperature and processed with a line-broadening factor of 50 Hz. Chemical shifts were calibrated using an external sample of tetrakistrimethylsilane (TKS). Solid-state ^{13}C NMR determination of the syringyl/guaiacyl ratio $(S/G)_{NMR}$ in fresh and decayed oak was made using fresh spruce sapwood (*Picea abies*) to calculate the guaiacyl content (*12*). Briefly, S/G values were measured

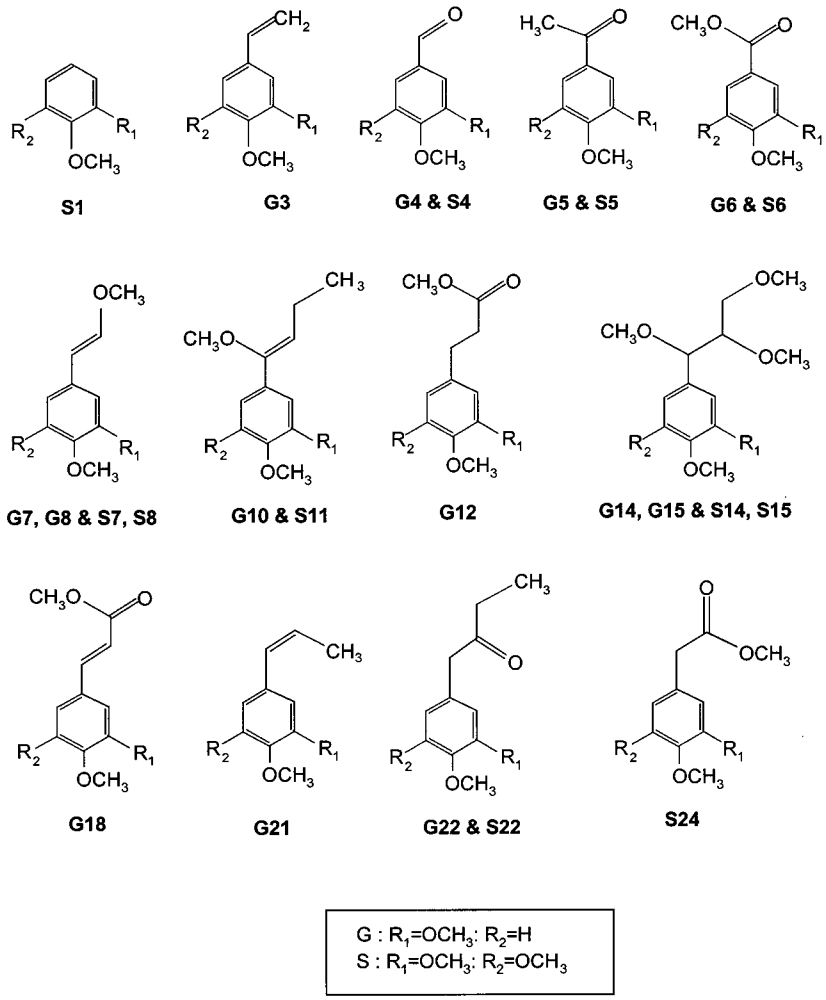

Figure 1. Structures of major thermochemolysis products after treatment of undegraded and degraded white oak with tetramethylammonium hydroxide.

Table 1. Bulk Compositions of Fresh and *L. edodes*-Decayed Oak Wood

time (months)	% N	% C	% H	% O	δ ^{13}C (‰)
0	0.29 ± 0.01	46.58 ± 0.06	6.01 ± 0.11	47.13	–27.0
30	0.28 ± 0.01	44.79 ± 0.04	5.56 ± 0.07	49.38	–25.2
40	0.29 ± 0.01	44.92 ± 0.03	5.46 ± 0.14	49.34	–26.4
66	0.20 ± 0.02	43.07 ± 0.03	5.54 ± 0.05	51.20	–27.9
76	0.23 ± 0.04	43.04 ± 0.15	5.26 ± 0.21	51.48	–26.6
77	0.22 ± 0.02	44.83 ± 0.03	5.68 ± 0.02	49.28	–26.0
101	1.23 ± 0.05	39.25 ± 0.03	4.61 ± 0.18	54.92	–25.3

from the dipolar dephased spectra with integration of the original spectrum (S + G) and the spruce wood-subtracted spectrum (S−G) between 120 and 160 ppm. The areas of S and G were normalized to an equal number of nonprotonated aromatic carbons by dividing the area of S by 4 and the area of G by 3 to calculate S/G ratios (*11*).

RESULTS

The elemental composition and stable carbon isotope values of fresh and decayed oak are presented in **Table 1**. The control oak had a carbon content of 46.6% (w/w), whereas all fungally degraded oak woods had carbon contents of <44.8% (w/w), with the lowest value equal to 39.3% (w/w) after 101 months of decay. In contrast, no significant changes in nitrogen content were observed between the control and inoculation times up to and including 40 months of growth. A decrease in nitrogen content of 0.6% (w/w) was observed for decay times up to and including 77 months (**Table 1**), and the nitrogen content clearly increased after 101 months of growth. However, overall, the nitrogen content remained lower than the content of all other elements. The hydrogen content of fresh oak was 6.0% (w/w); this generally decreased with growth of *L. edodes* to give a hydrogen content of 4.6% (w/w) after 101 months. The oxygen contents of fresh and decayed oak ranged from a minimum value of 47.1% (w/w) to a maximum value of 54.9% (w/w) (**Table 1**). All decayed oak woods had oxygen contents higher than those of their fresh counterparts.

Changes in the stable carbon isotopic signature from oak occurred with fungal growth (**Table 1**). The δ ^{13}C composition of the control was −27.0‰, which is similar to the result of previous measurements made on whole wood from white oak (*13*). Oak woods exhibited an enrichment in δ ^{13}C values upon fungal growth, with the exception of the 66-month time interval, at which it was depleted by 0.9‰ from the control (**Table 1**). A comparison of the δ ^{13}C values determined for fresh oak (−27.0‰) and *L. edodes* fungal mycelium (−23.8‰) shows that the mycelium is enriched by about 3.2‰.

The total ion current GC-MS traces for the flash pyrolysate of oak and oak treated with *L. edodes* are shown in **Figure 2**, and the peak assignments are given in **Table 2**. Chromatograms of fresh and decayed oak were dominated by lignin and polysaccharide pyrolysis products as well as nonspecific compounds such as toluene (**1**) and styrene (**5**). The pyrolysate of fresh oak shows several products of polysaccharides, identified as 3-furaldehyde (**3**), 2,3-dihydro-5-methylfuran-2-one (**10**), and

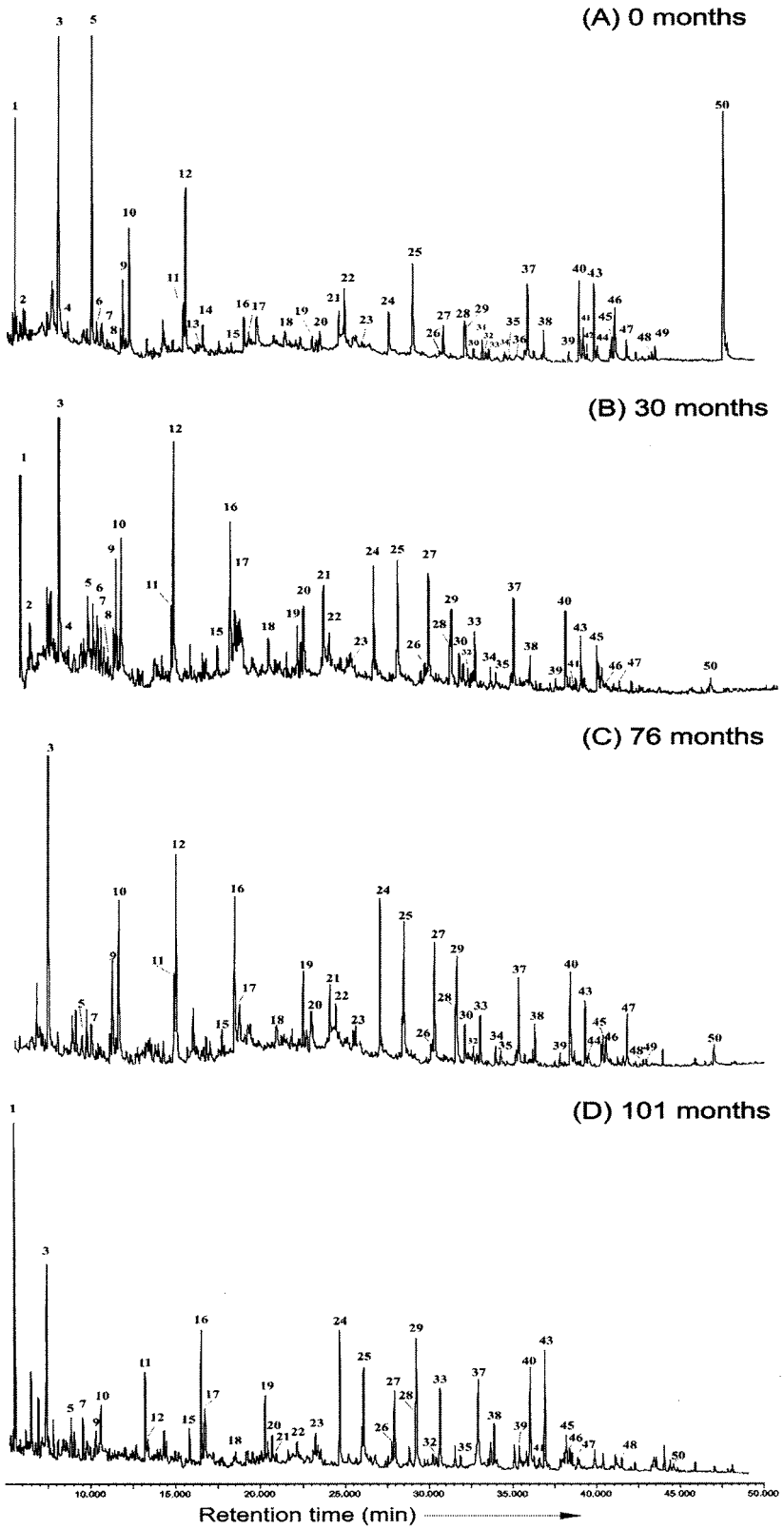

Figure 2. Partial chromatogram of the total ion current (TIC) of the pyrolysis products from (A) undegraded control white oak and white oak degraded for (B) 30, (C) 76, and (D) 101 months by *L. edodes.* Labels denote compounds listed in **Table 2**.

4-hydroxy-5,6-dihydro-(2*H*)-pyran-2-one (**12**), as well as minor amounts of the cellulose product 1,6-anhydro-β-D-glucopyranose (levoglucosan) (**36**). The lignin composition of fresh oak is comprised of syringyl (S) and guaiacyl (G) units with minor contributions of *p*-hydroxphenyl (H) moieties (**Figure 2A**). The major lignin pyrolysis products were identified as 2-methoxyphenol (**16**), 2,6-dimethoxyphenol (**25**), 4-methyl-2,6-dimethoxyphenol (**28**), 4-vinyl-2,6-dimethoxyphenol (**37**), 4-formyl-2,6-dimethoxyphenol (**40**), 2-methoxy-4-(prop-2-enal)phenol (**46**), and 2,6-dimethoxy-4-(prop-2-enal)phenol (**50**) (**Figure 2A**). The ratios of syringyl to guaiacyl lignin units (S/G) at the different stages of biodegradation are listed in **Table 3**. The $(S/G)_{pyrolysis}$ ratio displays an initial decrease from 2.6 in fresh oak to 0.80 after 30 months of decay; with longer decomposition times, this

Table 2. List of Pyrolysis Products

compd	assignment	characteristic ions	structure[a]
1	toluene	91, 92, 65	
2	(2*H*)-furan-2-one	84, 55	PS
3	3-furaldehyde	95, 96, 39	PS
4	ethylbenzene	91, 106, 65	
5	styrene	104, 103, 78	
6	cyclopent-1-ene,3–4-dione	96, 68, 54	PS
7	2-methyl-2- cyclopenten-1-one	96, 67, 53	PS
8	2-acetylfuran	95, 110, 43	PS
9	(5*H*)-furan-2-one	84, 55	PS
10	2,3-dihydro-5-methylfuran-2-one	98, 69, 55	PS
11	5,6-dihydropyran-(2*H*)-dione	112, 84, 56	PS
12	4-hydroxy-5,6-dihydro-(2*H*)-pyran-2-one	114, 58,85	PS
13	3-hydroxy-2-methyl-2-cyclopenten-1-one	112, 84, 71	PS
14	2-hydroxy-3-methyl-2-cyclopenten-1-one	112, 83, 69	PS
15	2-methylphenol	108, 107, 79	P—C
16	2-methoxyphenol	109, 124, 81	G
17	4-methylphenol	107, 108, 77	P—C
18	dihydroxypyran-1-one	114, 84, 56	PS
19	4-methyl-2-methoxyphenol	123, 138, 69	G—C
20	unknown	43, 69, 82, 116	PS
21	unknown	43, 55, 114	PS
22	2,5-dihydro-(1*H*)-pyrrole	68, 69, 43	PS
23	4-ethyl-2-methoxyphenol	152, 137, 109	G—C—C
24	4-vinyl-2-methoxyphenol	150, 135, 107	G—C═C
25	2,6-dimethoxyphenol	154, 139, 111	S
26	*cis*-2-methoxy-4-(prop-2-enyl)phenol	164, 149, 103	G—C═C—C
27	4-formyl-2-methoxyphenol	152, 151, 109	G—CHO
28	4-methyl-2,6-dimethoxyphenol	168, 153, 125	S—C
29	*trans*-2-methoxy-4-(prop-2-enyl)phenol	164, 149, 103	G—C═C—C
30	4-ethanal-2-methoxyphenol	137, 166, 122	G—C—CHO
31	4-propynyl-2-methoxyphenol	147, 162, 119	G—C≡C
32	unknown	147, 162, 119	
33	4-acetyl-2-methoxyphenol	151, 166, 123	G—CO—C
34	4-ethyl-2,6-dimethoxyphenol	167, 182, 137	S—C—C
35	2-methoxy-4-(propan-2-one)phenol	137, 180, 122	G—C—CO—C
36	1,6-anhydro-β-D-glucopyranose	60, 57, 73	PS
37	4-vinyl-2,6-dimethoxyphenol	180, 165, 137	S—C═C
38	2,6-dimethoxy-4-(prop-1-enyl)phenol	194, 119, 91	S—C—C═C
39	*cis*-2,6-dimethoxy-4-(prop-2-enyl)phenol	194, 119, 91	S—C═C—C
40	4-formyl-2,6-dimethoxyphenol	181, 182, 111	S—CHO
41	4-propynyl-2,6-dimethoxyphenol	192, 147, 119	S—C≡C
42	unknown	192, 147, 119	
43	*trans*-2,6-dimethoxy-4-(prop-2-enyl)phenol	194, 119, 91	S—C═C—C
44	4-ethanal-2,6-dimethoxyphenol	167, 196, 123	S—C—CHO
45	4-acetyl-2,6-dimethoxyphenol	181, 196, 153	S—CO—C
46	2-methoxy-4-(prop-2-enal)phenol	178, 145, 137	G—C═C—CHO
47	2,6-dimethoxy-(propan-2-one)phenol	167, 210, 123	S—C═C—CHO
48	2,6-dimethoxyphenol-4-(propan-3-one)	181, 210, 151	S—CO—C—C
49	2,6-dimethoxy-4-(prop-1-en-3-one)	181, 208, 153	S—CO—C═C
50	2,6-dimethoxy-4-(prop-2-enal)phenol	208, 165, 137	S—C═C—CHO

[a] Abbreviations: PS, polysaccharide; G, 2-methoxylphenol (guaiacyl); S, 2,6-dimethoxyphenol (syringyl).

Table 3. Qualitative Changes in the Distribution of Lignin-Derived Pyrolysis Products after Attack by *L. edodes*[a]

decay time (months)	$(S/G)_{pyrolysis}$	G:3-to-G lignin	S:3-to-S lignin
0	2.60	0.46	0.49
30	0.80	0.20	0.26
40	0.75	0.19	0.30
66	0.75	0.19	0.30
76	0.73	0.23	0.23
77	0.95	0.13	0.17
101	0.96	0.31	0.22

[a] All ratios are calculated using the integration of the relevant peaks in the TICs from Py-GC-MS.

value varied only slightly (**Table 3**). The relative intensity of 2,6-dimethoxy-4-(prop-2-enal)phenol (**50**) decreased relative to that of other products upon 30 months of decay (compare panels A and B of **Figure 2**). Changes in the relative abundance of lignin units with complete alkyl side chains were also evident from the decrease in G:3/G and S:3/S ratios (**Table 3**). **Figure 3A** shows the major thermochemolysis products from fresh oak, which were identified as 3,4,5-trimethoxybenzaldehyde (**S4**), 3,4,5-trimethoxyacetophenone (**S5**), and 3,4,5-trimethoxybenzoate (**S6**), as well as cis and trans isomers of 1-(3,4,5-trimethoxyphenyl)-2-methoxyethylene (**S7**, **S8**). Other important products included 3,4-dimethoxybenzaldehyde (**G4**) and the enantiomers of 1-(3,4,5-trimethoxyphenyl)-1,2,3-trimethoxypropane (**S14**, **S15**) (**Figure 3A**). The threo/erythro forms of 1-(3,4,5-trimethoxyphenyl)-1,2,3-trimethoxypropane (**G14**, **G15**) and **S14**, **S15** are derived from guaiacyl and syringyl moieties, retaining complete propyl ether interunit linkages.

After 30 months of decay by *L. edodes*, the main thermochemolysis products were 3,4-dimethoxybenzoate (**G6**) and **S6** (**Figure 3B**−**D**), and the amounts of **S5**, **S7**, **S8**, *trans*-1-(3,4,5-trimethoxyphenyl)methoxyprop-1-ene (**S11**), **S14**, and **S15** decreased relative to other products. The ratio of dimethoxy-

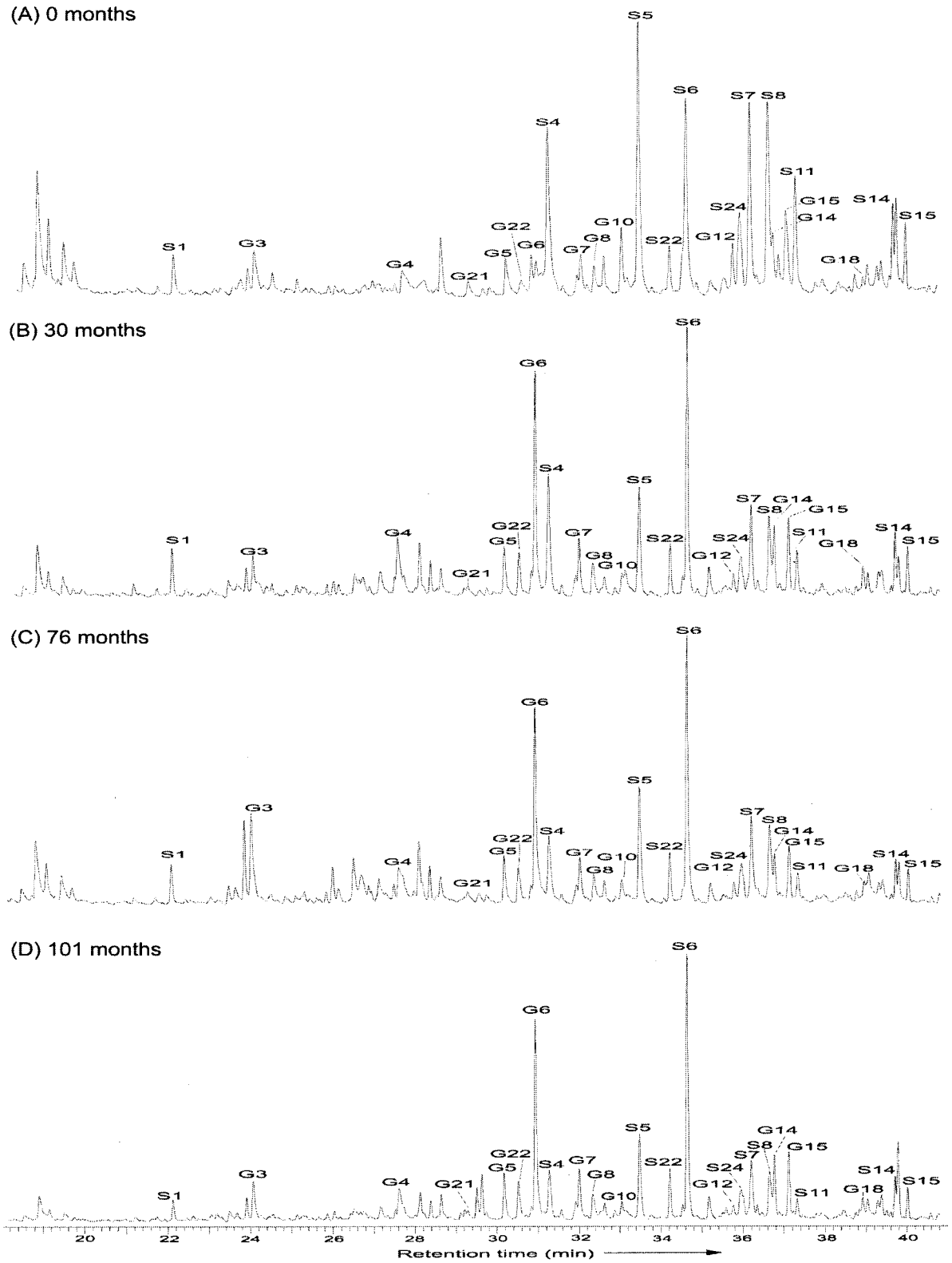

Figure 3. Partial chromatogram of the total ion current (TIC) of the thermochemolysis products from (A) undegraded control white oak and white oak degraded for (B) 30, (C) 76, and (D) 101 months by *L. edodes.* Labels denote structures shown in **Figure 1**.

phenol to monomethoxphenol derivatives, determined by the TMAH thermochemolysis method $(S/G)_{TMAH}$, for fresh oak was 2.1, similar to previous measurements made on lignin from oak using alkaline nitrobenzene oxidation (*12*). The S/G values decreased to 1.2 after 30 months of growth of *L. edodes*; for decay times greater than 30 months, the S/G value remained at ~1 (**Figure 4A**). The $(Ad/Al)_G$, $(Ad/Al)_S$, and Γ values increased upon fungal decay (**Figure 4A**,**B**). The $(Ad/Al)_G$ and $(Ad/Al)_S$ values of the fresh oak were 0.9 and 1.1, respectively; after 30 months, $(Ad/Al)_G$ was 3.7 and $(Ad/Al)_S$ was 2.3 (**Figure 4B**), and after 40 months, $(Ad/Al)_G$ was 5.9 and $(Ad/Al)_S$ was 3.4 (**Figure 4B**). With longer decay times (66 months), $(Ad/Al)_G$ decreased but always remained higher than its undegraded counterparts. Maximum $(Ad/Al)_G$ values were observed after

Table 4. Distribution of Carbon in Fresh and *L. edodes*-Degraded Oak Wood as a Percentage of the Total Carbons from ^{13}C NMR Spectra

	%carbon						
growth time (months)	acetyl 5–30 ppm	methoxyl 50–60 ppm	carbohydrate (C-2, C-3, C-4, C-5, and C-6 of cellulose and xylans) 60–90 ppm	carbohydrate (C-1 of cellulose, xylans, and aliphatic lignin) 95–110 ppm	aromatic lignin 110–160 ppm	carboxyl/carbonyl 160–210 ppm	syringyl/guaiacyl $(S/G)_{NMR}$
0	4.0	11.5	56.0	12.5	10.5	5.5	1.46
30	4.5	14.0	49.5	11.0	16.0	4.5	1.11
40	4.5	12.5	52.5	11.0	13.5	5.5	1.12
66	4.0	10.5	56.0	12.0	11.0	6.5	0.88
76	3.5	11.0	55.5	12.5	12.5	5.5	0.75
77	4.0	10.5	55.0	12.0	12.5	6.0	0.78
101	7.5	16.0	38.5	8.5	20.5	8.5	0.69

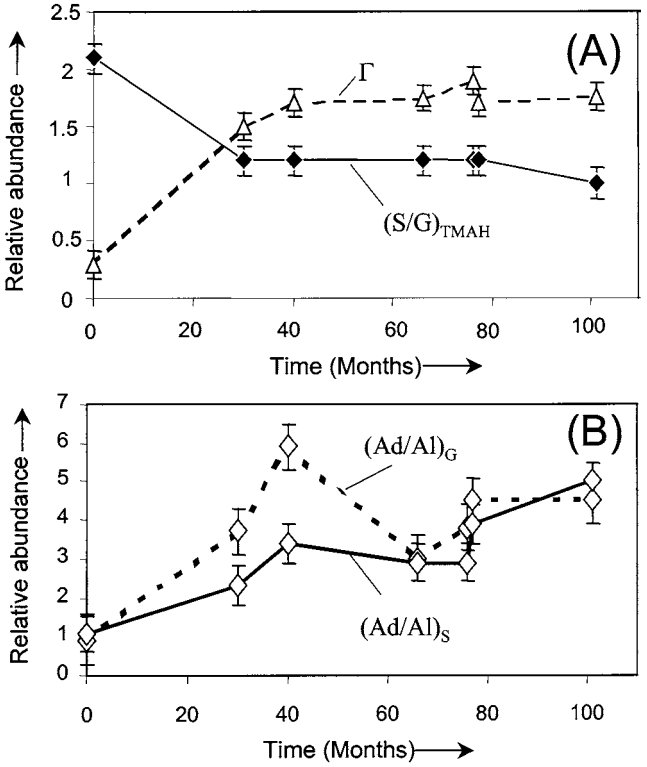

Figure 4. Time-dependent changes in (A) 3,4-dimethoxybenzoate relative to the summed amounts of threo and erythro forms of 1-(3,4-dimethoxyphenyl)-1,2,3-trimethoxypropanone (Γ) and syringyl/guaiacyl derivatives $(S/G)_{TMAH}$, (B) 3,4-dimethoxybenzoate/3,4-dimethoxybenzaldehyde $(Ad/Al)_G$, and 3,4,5-trimethoxybenzoate/3,4,5-trimethoxybenzaldehyde $(Ad/Al)_S$ in white oak during growth of *L. edodes*.

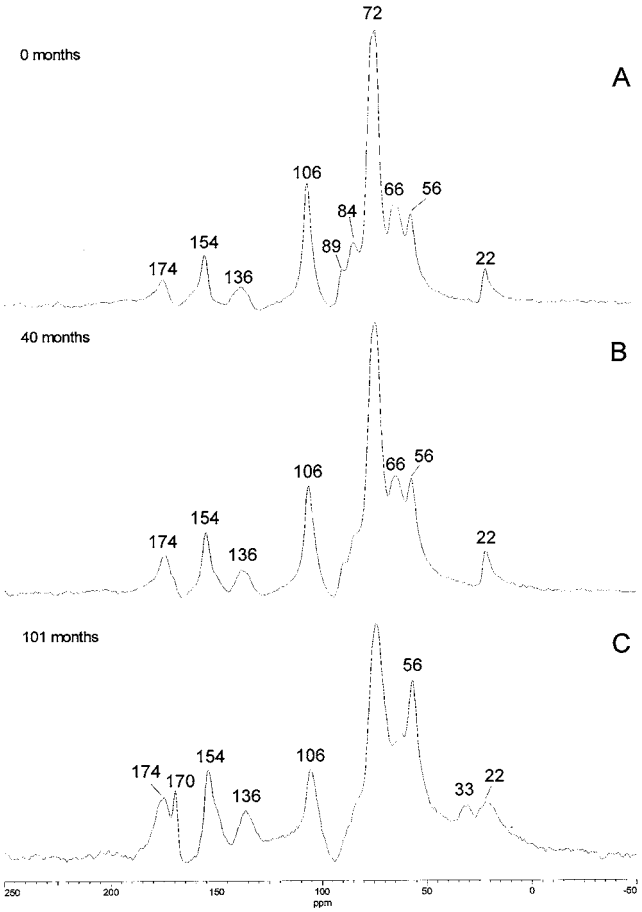

Figure 5. Solid-state ^{13}C CP/MAS NMR spectra for (A) undegraded control white oak and white oak decayed for (B) 40 and (C) 101 months by *L. edodes*.

40 months of decay; in contrast, the highest $(Ad/Al)_S$ of 5 was found at 101 months of decomposition (**Figure 4B**). The Γ value for fresh oak was 0.3; after 30 and 40 months, the Γ values were 1.5 and 1.7, respectively (**Figure 4A**). Within experimental error, the Γ values showed little variation for decomposition times greater than 40 months, with the exception of a small increase after 76 months.

Conventional CPMAS ^{13}C NMR spectra of fresh oak and oak following *L. edodes* growth (40 and 101 months) are presented in **Figure 5**. The control oak is dominated by resonances in the 60−110 ppm region from polysaccharides. The resonance at 72 ppm is from C-2, C-3, and C-5 carbons of cellulose and xylans (*14*). Both crystalline and amorphous cellulose are present in fresh oak, as shown by the peaks at 84 and 89 ppm, respectively (*15*). Additional cellulose resonances are at 66 (C-6) and 106 ppm (C-1) (**Figure 5A**). The distinct single peak at 106 ppm confirmed that the main carbohydrate in oak was cellulose type I, although there is undoubtedly some overlap with C-1 carbons of xylans at 103 ppm (*16*). There are signals at 60, 72, and 84 ppm in the ^{13}C NMR spectra of lignin from naturally decayed white oak, assigned to carbon atoms in ether and secondary alcohol functional groups (*14*). However, in unaltered woods, the contribution of carbon from lignin to the 60−110 ppm region is low in comparison to that from the polysaccharides (*17*). Therefore, the areas of the peaks at 66, 72, 84, 89, and 106 ppm provide an estimate of the relative amounts of polysaccharides (**Table 4**). Fresh oak was composed of 69% carbohydrate carbon; at 30 and 40 months, the amounts of polysaccharide carbon were 61% and 64%, respectively. Oak after 66, 76, and 77 months of treatment with *L. edodes* exhibited a decrease in carbohydrate content of only ∼2−3% compared to the undecayed counterpart (**Table 4**). At 101

months of decay, the polysaccharide content was 47%, which is equivalent to an overall decrease of 22% (**Table 4**). The amount of carbohydrate carbon decreased to an average of 62.5% over the entire cropping period (30−101 months).

Fresh and decayed oak samples exhibit resonances between 110 and 160 ppm, attributed to carbon in aromatic rings from lignin (**Figure 5**). The broad, distinct peak at 136 ppm is from C-1 carbons of aromatic rings, and the peak at 154 ppm is from C-3 and C-5 carbon atoms in syringyl (**Figure 5**). Other lignin resonances include the shoulder at 148 ppm, assigned to C-3 and C-5 carbons in guaiacyl units, which are O-alkylated. Aromatic carbon in fresh oak was 10.7%; this generally increased with mushroom growth to give an aromatic lignin content of 20.6% after 101 months, which is equivalent to a 10.1% increase from the fresh oak (**Table 4**). The resonance at 174 ppm is attributed mainly to acetate groups in xylans and carbonyl groups in lignin. The carboxyl/carbonyl content of fresh oak wood was 5.6% (**Table 4**). Changes in the carboxyl/carbonyl carbon content (160−200 ppm) were independent of growth time (**Table 4**). The highest carbonyl/carboxyl contents were observed at 101 months of growth. However, the appearance of a new peak at 33 ppm (101 months), which can be assigned to methylene groups in proteins, suggested that amide carbons could also contribute to the peak at 174 ppm (**Figure 5C**). The resonance at 56 ppm is from aryl methoxyl carbons of lignin, which comprised 11.4% of the total carbon in fresh oak. The methoxyl content varied in a nonsystematic fashion throughout mushroom cultivation (**Table 4**). The S/G value of fresh oak, as determined by solid-state ^{13}C NMR, was 1.46 (**Table 4**). This decreased to a value of 1.11 after 30 days and continued to slowly decrease to a value of 0.69 after 101 months of biodegradation (**Table 4**).

DISCUSSION

The increase in C/N ratio from 160 in fresh oak to 203 after 77 months of mushroom growth is consistent with a decomposition of carbon components by *L. edodes*. Similarly, C/N ratios increased from 14.1 in mushroom compost to 16.3 upon growth of *Agaricus bisporus* (*18*). The decrease in C/N ratio to 32 after 101 months is explained by the incorporation of nitrogen-rich fungal mycelium and simultaneous carbon loss (**Table 1**) (*19*). It has been documented that soils amended with wood and bark with high C/N ratios can cause an initial nitrogen starvation of crop plants (*20*). In this light, it is clear that only oak logs which have been heavily decayed by *L. edodes* (e.g., 101 months) can be considered as a viable compost component for field crop application.

The accumulation of oxygen in woods and wheat straw decayed by white-rot fungi has been previously documented (*21*−*23*). The pathway for the oxidative degradation of lignin by isolated extracellular enzymes from *L. edodes* has been proposed (*4*−*7*). In these studies, the degradation products of veratryl alcohol, vanillyl alcohol, and phenolic lignin model compounds having carbon−carbon interunit bonds were analyzed using GC-MS and, in some instances, ^{1}H NMR and IR spectroscopy. Aromatic carboxylic acids were formed by a sequence of autoxidations on alkyl side chains. In the present study, the increase in oxygen content in degraded oak woods is consistent with the oxidation of the lignin observed following incubation of model compounds with enzymes extracted from the extracellular fluid of *L. edodes*.

The overall increase in ^{13}C values by an average of 0.8‰ in oak upon mushroom growth was not expected (**Table 1**). It is well established that microbial degradation of vascular plants causes ^{13}C depletions due to the preferential degradation of isotopically heavy cellulose and xylans compared to isotopically lighter lignin (*24*, *25*). However, fresh oak gave a δ ^{13}C value of −27‰, and *L. edodes* mycelium gave a δ ^{13}C value of −23.8‰. Other workers have documented that basidocarps of wood-decomposing fungi are enriched by about 3.5‰ compared to the wood upon which they grow (*26*). The ^{13}C enrichment of oak wood with mushroom growth is therefore consistent with an increase in residual fungal biomass.

Pyrolysis of plant polysaccharides results in major thermal transformations and secondary reactions; thus, the polysaccharides identified in this study cannot be unequivocally related to precursors in the original macromolecule and are of limited diagnostic value. The poorly resolved nature of the cellulose pyrolysis product 1,6-anhydro-β-D-glucopyranose (**36**) in fresh oak also illustrates chromatographic limitations of the technique, and for these reasons an estimate of carbohydrate content was not undertaken (*27*). Lignin-derived pyrolysis products from the control sample consisted mainly of syringyl and guaiacyl phenols and, to a lesser extent, *p*-hydroxyphenyl moieties, which is consistent with lignin from angiosperm woods including oak species (*28*). The product 2,6-dimethoxy-4-(prop-2-enal)phenol (**50**) was identified in large amounts in fresh oak relative to other methoxyphenols (**Figure 2A**). Other workers have observed the pyrolytic dehydroxylation of sinapyl alcohol to 2,6-dimethoxy-4-(prop-2-enal)phenol and dimethoxypropenyl phenols (*11*, *29*). Therefore, 2,6-dimethoxy-4-(prop-2-enal)phenol (**50**) and the products **38**, **39**, and **43** may be derived from the thermal alteration of the primary product sinapyl alcohol (2,6-dimethoxy-4-(1-hydroxyprop-2-enyl)phenol and do not necessarily reflect primary lignin structure in oak. Similarly, the pyrolysis products 4-vinyl-2-methoxyphenol (**24**) and 4-vinyl-2,6-dimethoxyphenol (**37**) are generated from either the pyrolytic decarboxylation of ferulic and sinapic acids, which links xylans to lignin, or the decomposition of related lignin alcohol (*30*).

The overall chemical composition of oak wood was altered with growth of *L. edodes*, as revealed by analytical pyrolysis. The decrease in S/G ratio with cultivation time is probably caused by an initial (40 months) preferential decay of S units, after which the S/G ratio stabilizes. The decrease in S/G ratio upon fungal decomposition is explained by syringyl moieties being more susceptible to degradation because they have fewer aryl−aryl bonds and have a lower redox potential than their guaiacyl counterparts (*31*). The large decrease in S/G values upon decay by *L. edodes* contrasts with observations from an earlier study, where analytical pyrolysis (Py-GC-MS) of beech wood treated with *L. edodes* for 98 days revealed a moderate decrease in S/G values from 1.4 to 1.3 upon decay (*9*). These differences are probably best explained by the longer decay times used in this current study. Further insights into lignin degradation during cultivation of *L. edodes* are supported by the time-dependent decrease in G:3/G and S:3/S ratios (**Table 3**). One plausible explanation for this trend is lignin side chains shortening; this is entirely consistent with the known chemical modifications to lignin induced by many white-rot fungi (*23*, *32*, *33*). However, the decrease in lignin units with complete C_3 side chains was not accompanied by a concomitant increase in lignin phenols with oxidized side chains, as has been observed during incubation of veratryl alcohol and vanillyl alcohol with *L. edodes* extracellular enzymes (*4*). One possible explanation for the trend in this work may be that *L. edodes* mediated oxidative side-chain cleavage, which at its final stage yields carboxylic acids, which are not readily GC amenable (*11*).

Thermochemolysis of fresh oak gave an S/G of 2.1, whereas pyrolysis of fresh oak gave an S/G of 2.6. This difference in S/G ratios is probably due to thermolytic as compared to chemolytic mechanisms of macromolecular depolymerization. Lignin pyrolysis produts are derived from the cleavage of both ether and aryl−aryl linkages; in contrast, thermochemolysis acts mainly to break propyl−aryl ether linkages, where there are adjacent hydroxyl groups on the alkyl side chain (*34*, *35*). A comparison of S/G ratios determined from the peak areas of pyrolysis and thermochemolysis products shows similar overall decreases with fungal growth to values of ∼1 (**Table 3**; **Figure 4A**).

Application of thermochemolysis in microbial biodegradation studies requires use of both Ad/Al and Γ parameters to infer the extent of oxidative side-chain cracking, since increased Ad/Al values can potentially result from dehydration of hydroxyl groups on lignin side chains, lowering amounts of aldehyde without an increase in the amount of acid (*33*). The increases in $(Ad/Al)_G$ and $(Ad/Al)_S$ values upon decay suggest that the fungus *L. edodes* degraded both guaiacyl and syringyl units via oxidative cleavage of the Cα−Cβ at the Cα atom, to yield aldehydes which are further oxidized to carboxylic acid in a manner similar to that in other edible fungi (*36*). Comparison of the S/G values with $(Ad/Al)_G$ and $(Ad/Al)_S$ values reveals that, for decay times up to but not greater than 76 months, the $(Ad/Al)_G$ values are greater than $(Ad/Al)_S$ values; this is probably caused by the more rapid decay and complete loss of syringyl units relative to guaiacyl units, as suggested by the decrease of the S/G ratio (**Figure 4A**,**B**). The increase in Γ parameters provides additional evidence of oxidative cleavage of propyl ether interunit linkages and associated degradation of guaiacyl moieties within a complete glycerol side chain; however, this process appears to be inhibited for decomposition times greater than 40 months (**Figure 4A**). The oxidative mechanism of lignin degradation has also been investigated by incubating model guaiacyl lignin dimers with manganese(II) peroxidase isolated from *L. edodes*. The biphenyl model compound, dihydrocresol, and 3,3-dihydroxy-4,4-dimethoxy-6,6-dimethyldiphenylmethane were decayed via oxidative cleavage of the side chain (*6*). Therefore, the oxidative side-chain alterations observed in this present work could have also been initiated by Mn peroxidases secreted by *L. edodes*.

^{13}C NMR spectra of fresh and degraded oak show that cellulose and xylans were the major structural constituents of oak wood throughout the entire cultivation period. The polysaccharide content of oak remained remarkably high throughout the early and middle stages of growth and only became heavily decayed after 101 months. In the ^{13}C NMR spectra of spruce and birch wood, there are resonances at 89 and 84 ppm which can be assigned to C-4 crystalline cellulose and C-4 amorphous cellulose (*37*, *38*). The diminished resolution of both C-4 cellulose peaks with cultivation of *L. edodes* (**Figure 5A**−**C**) suggested that there was no preference for removal of the amorphous component of oak. Other workers have also reported that biodegradation of beech wood by *L. edodes* does not effect a preferential decay of amorphous non-cellulosic xylans (*9*).

The occurrence of new resonances at 33 and 170 ppm from lipid and amide carbon in protein after 101 months of decay (**Figure 5C**) suggested a source of fungal biomass. This concept is consistent with previous ^{13}C NMR spectra of edible mushrooms, which show resonances from polysaccharides (105, 90 ppm) and protein (170, 33, 55, 20 ppm) components (*39*). Furthermore, the decline in the C/N ratio at the 101-month interval supports the hypothesis that fungal mycelium became incorporated into the cell wall of oak. In addition, the nonsystematic changes in methoxyl content are not caused by demethylation reactions, such as those observed during brown-rot degradation, but are explained by the incorporation of proteins from fungal mycelium which contribute to the signal at ∼56 ppm (*33*, *39*).

The S/G values for fresh and decayed oak, as determined by solid-state ^{13}C NMR (1.5−0.7), were lower than those calculated from pyrolysis and thermochemolysis data (**Tables 3** and **4**; **Figure 4A**). This phenomenon is explained by the higher frequency of guaiacyl units linked by aromatic carbon−carbon bonds (condensed structures) which are not generally cleaved by thermochemolysis and, on the basis of bond energies, are less thermally labile than ether-type linkages (*34*, *35*). The solid-state ^{13}C NMR S/G values show a gradual decrease from 0 to 101 months, as compared to the more rapid change determined by pyrolysis and thermochemolysis during the first 30 months (**Tables 3** and **4**; **Figure 4A**). This suggests that syringyl structures linked via propyl ether interunit bonds are rapidly degraded for the first 30 months of growth. However, with longer decay times, the syringyl moieties linked by carbon−carbon bonds are decayed.

The increase in aromatic carbon content after fungal attack (**Table 4**) supports the view that *L. edodes* decayed the polysaccharide components in preference to the lignin. Therefore, the NMR spectra suggest that cellulose, xylans, and lignin were decayed in parallel during cultivation of the edible fungus. Complementary evidence from analytical pyrolysis and thermochemolysis revealed that enzymes secreted by *L. edodes* removed syringyl moieties in preference to guaiacyl units and cleaved the Cα−Cβ bonds in lignin side chains. Future studies in our laboratories will examine the effect of *L. edodes* on the solvent-insoluble constituents of bark from oak using the pyrolytic, thermolytic, and spectroscopic techniques examined in the present study.

ACKNOWLEDGMENT

The authors thank Hilary Sloane for bulk C isotope measurements (National Isotope Geosciences Laboratory) and Ian Harrison (British Geological Survey) for helpful comments regarding the manuscript. Samples were collected by Tom Kimmons and co-workers, Ozark Speciality, Arkansas. This paper is published by permission of the Executive Director, British Geological Survey (NERC).

LITERATURE CITED

(1) Kirk, T. K.; Farrell, R. L. Enzymatic "combustion": The microbial degradation of lignin. *Annu. Rev. Microbiol*. **1987**, *6*, 465−505.

(2) Orth, A. B.; Royse D. J.; Tien, M. Ubiquity of lignin-degrading peroxidases among various wood-decaying fungi. *Appl. Environ. Microbiol*. **1993**, *59*, 4017−4023.

(3) Makkar, R. S.; Tsuneda, A.; Tokuyasu, K.; Mori, Y. *Lentinula edodes* produces a multicomponent protein complex containing manganese (II)-dependent peroxidase, laccase and beta-glucosidase. *FEMS Microbiol. Lett.* **2001**, *2*, 175−179.

(4) Crestini, C.; Giovannozzi Sermanni, G. Aromatic ring oxidation of vanillyl and veratryl alcohols by *Lentinus edodes*: Possible artifacts in the lignin peroxidase and veratryl alcohol oxidase assays. *J. Biotechnol.* **1995**, *39*, 175−179.

(5) D'Annibale, A.; Crestini, C.; Di Mattia, E.; Giovannozzi Sermanni, G. Veratryl alcohol oxidation by manganese-dependent peroxidase from *Lentinus edodes*. *J. Biotechnol*. **1996**, *48*, 231−239.

(6) Crestini, C.; D'Annibale, A.; Giovannozzi Sermanni, G.; Saladino, R. The reactivity of phenolic and non-phenolic residual kraft lignin model compounds with Mn(II)-peroxidase from *Lentinula edodes*. *Bioorg. Med. Chem.* **2000**, *8*, 433−438.

(7) Crestini, C.; Giovannozzi Sermanni, G.; Argyropoulos, D. S. Structural modifications induced during biodegradation of wheat lignin by *Lentinula edodes*. *Bioorg. Med. Chem*. **1998**, *6*, 967−973.

(8) Nimz, H. H.; Robert, D.; Faix, O.; Nemr, M. Carbon-13 NMR spectra of lignins: Structural differences between lignins of hardwoods, softwoods, grasses and compression wood. *Holzforschung* **1981**, *35*, 16−26.

(9) Faix, O.; Bremer, J.; Schmidt, O.; Stevanovic, T. J. Monitoring of chemical changes in white-rot degraded beech wood by pyrolysis-gas chromatography and Fourier transform infrared spectroscopy. *J. Anal. Appl. Pyrolysis* **1991**, *21*, 147−162.

(10) Hedges, J. I.; Cowie, G. L.; Ertel, J. R.; Barbour R. J.; Hatcher, P. G. Degradation of carbohydrates and lignins in buried woods. *Geochim. Cosmochim. Acta* **1985**, *49*, 701−711.

(11) Ralph, J.; Hatfield, D. Pyrolysis-GC-MS characterization of forage materials. *J. Agric. Food. Chem*. **1991**, *39*, 1426−1437.

(12) Manders, W. F. Solid-state ^{13}C NMR determination of syringyl/guaiacyl ratio in hardwoods. *Holzforschung* **1987**, *41*, 13−1.

(13) Schleser, G. H.; Frielingsdorf, J.; Blair, A. Carbon isotope behaviour in wood and cellulose during artificial ageing. *Chem. Geol.* **1999**, *158*, 121−130.

(14) Hatcher, P. G. Chemical structural studies of natural lignins by dipolar dephasing soild-state ^{13}C nuclear magnetic resonance. *Org. Geochem*. **1987**, *11*, 31−39.

(15) Gil, A. M.; Pascoal Neto, C. Solid-sate NMR studies of wood and other lignocellulose materials. *Annu. Rep. NMR Spectrosc*. **1999**, *37*, 75−117.

(16) Atalla, R. H.; VanderHart, D. L. The role of solid state ^{13}C NMR spectroscopy in studies of the nature of native celluloses. *Solid State Nucl. Magn. Reson*. **1999**, *15*, 1−9.

(17) Maunu, S. L. NMR studies of wood and wood products. *Prog. Nucl. Magn. Reson.* **2002**, *40*, 151−174.

(18) Chen, Y.; Chefetz, B.; Rosario, R.; van Heemest, J. D. H.; Romaine C. P.; Hatcher, P. G. Chemical nature and composition of compost during mushroom growth. *Compost Sci. Util.* **2000**, *8*, 347−359.

(19) Vane, C. H.; Martin, S. C.; Snape, C.; Abbott, G. D. Degradation of lignin in wheat straw during growth of the Oyster mushroom (*Pleurotus ostreatus*) using off-line thermochemolysis with tetramethylammonium hydroxide and solid state ^{13}C NMR. *J. Agric. Food. Chem*. **2001**, *49*, 2709−2716.

(20) Harkin, J. M.; Rowe, J. W. *Bark and its possible uses*; USDA Forest Serv. Res. Note FPL-091; Forest Products Laboratory: Madison, WI, 1971; 55 pp.

(21) Hedges, J. I.; Blanchette, R. A.; Weliky, K.; Devol, A. H. Effects of fungal degradation on the CuO oxidation products of lignin: A controlled laboratory study. *Geochim. Cosmochim. Acta* **1988**, *52*, 2717−2726.

(22) Goñi, M. A.; Nelson, B.; Blanchette, R. A.; Hedges, J. I. Fungal degradation of wood lignins: Geochemical perspectives from CuO-derived phenolic dimers and monomers. *Geochim. Cosmochim. Acta* **1993**, *57*, 3985−4002.

(23) Vane, C. H. The molecular composition of lignin in spruce decayed by white-rot fungi (*Phanerochaete chrysosporium* and *Trametes versicolor*) using pyrolysis-GC-MS and thermochemolysis with tetramethylammonium hydroxide. *Int. Biodet. Biodeg*. **2002**, *51*, 67−75.

(24) Benner, R.; Fogel, M. L.; Sprague E. K.; Hodson, R. E. Depletion of ^{13}C in lignin and its implications for carbon stable isotope studies. *Nature* **1987**, *329*, 708−710.

(25) Deines, P. The isotopic composition of reduced organic carbon. In *Handbook of Environmental Isotopic Geochemistry. The Terrestrial Environment*; Fitz, P., Fontes, J. C., Eds.; Elsevier: Amsterdam, 1980; Vol. 1, pp 329−406.

(26) Kohzu, A.; Yoshioka, T.; Ando, T.; Takahashi, M.; Koba, K.; Wada, E. Natural ^{13}C and ^{15}N abundance of field-collected fungi and their ecological implications. *New Phytol.* **1999**, *144*, 323−330.

(27) Saiz-Jimenez, C. Analytical pyrolysis of humic substances: Pitfalls, limitations, and possible solutions. *Environ. Sci. Technol.* **1994**, *28*, 1773−1780.

(28) Saiz-Jimenez, C.; Boon, J. J.; Hedges, J. I.; Hessels, J. K. C.; De Leeuw, J. W. Chemical characterization of recent and buried woods by analytical pyrolysis: Comparison of pyrolysis data with ^{13}C and wet chemical data. *J. Anal. Appl. Pyrolysis* **1987**, *11*, 437−450.

(29) Van der Hage, E. R. E.; Mulder, M. M.; Boon, J. J. Structural characterization of lignin polymers by temperature-resolved in source pyrolysis-mass-spectrometry and curie point pyrolysis-gas chromatography/mass spectrometry. *J. Anal. Appl. Pyrolysis* **1993**, *25*, 149−183.

(30) Mulder, M. M.; Pureveen, J. B.; Boon, J. J.; Martinez, A. T. An analytical pyrolysis mass spectrometry study of *Eucrphia cordifolia* wood decayed by white rot and brown rot fungi. *J. Anal. Appl. Pyrolysis* **1991**, *19*, 175−191.

(31) Tai, D.; Terazawa, M.; Chen, C.-L.; Chang, H-m.; Kirk, T. K. Biodegradation of guaiacyl and guaiaicyl-syringyl lignins in wood *by Phanerochaete chrysosporium.* In *Recent advances in lignin biodegradation research: fundamentals and biotechnology*; Higuchi, T., Chang, H-m., Kirk, T. K., Eds.; Uni. Publishers Co. Ltd.: Tokyo, Japan, 1983; pp 44−63.

(32) del Río, J. C.; Gutiérrez, A.; Martínez, M. J.; Martínez, A. T. Py-GC/MS study of *Eucalyptus globulus* wood treated with different fungi. *J. Anal. Appl. Pyrolysis* **2001** *58*−*59*, 441−452.

(33) Filley, T. R.; Hatcher, P. G.; Shortle, W. C.; Praseuth, R. T. The application of ^{13}C-labeled tetramethylammonium hydroxide (^{13}C-TMAH) thermochemolysis to the study of fungal degradation of wood. *Org. Geochem*. **2000**, *31*, 181−198.

(34) Evans, R.; Milne, T.; Soltys, M. Direct mass spectrometry studies of the pyrolysis of carbonaceous fuels III primary pyrolysis of lignin. *J. Anal. Appl. Pyrolysis* **1986**, *22*, 147−162.

(35) Filley, T. R.; Minard, R. D.; Hatcher, P. G. Tetramethylammonium hydroxide (TMAH) thermochemolysis: proposed mechanisms based upon the application of ^{13}C-labeled TMAH to a synthetic model lignin dimer. *Org. Geochem*. **1999**, *30*, 607−621.

(36) Vane, C. H.; Abbott, G. D.; Head, I. M. The effect of fungal decay (*Agaricus bisporus*) on wheat straw lignin using pyrolysis-GC-MS in the presence of tetramethylammonium hydroxide (TMAH). *J. Anal. Appl. Pyrolysis* **2001**, *60*, 69−78.

(37) Hortling, B.; Forsskåhl, I.; Janson, J.; Sundquist, J.; Viikari, L. Investigations of fresh and biologically decayed birch. *Holzforschung* **1992**, *46*, 9−19.

(38) Sosanwo, O. A.; Fawcett, A. H.; Apperley, D. ^{13}C CP-MAS NMR spectra of tropical hardwoods. *Polym. Int*. **1995**, *36*, 247−259.

(39) Pizzoferrato, L.; Manzi, P.; Bertocchi, F.; Fanelli, C.; Rotilio, G.; Paci, M.; Solid-state C-^{13}CP MAS NMR spectroscopy of mushrooms gives directly the ratio between proteins and polysaccharides. *J. Agric. Food Chem.* **2000**, *48*, 5484−5488.

Received for review September 4, 2002. Revised manuscript received November 27, 2002. Accepted November 29, 2002.

JF020932H